Journal of Fluorine Chemistry 267 (2023) 110104

Contents lists available at ScienceDirect

Journal of Fluorine Chemistry

journal homepage: www.elsevier.com/locate/fluor

Short Communication

Bifurcated hydrogen bonding to fluorine in an all *cis*-difluoro-hydroxy array

Muyuan Wang, Roseann K. Sachs [1], Stefan Andrew Harry, Eric Holt, Maxime A. Siegler, Thomas Lectka [*]

Department of Chemistry, Johns Hopkins University, 3400 North Charles St., Baltimore, MD, 21218, United States

ARTICLE INFO

Keywords:
Bifurcated hydrogen bonding
Fluorination
Difluorination
Hydroxy-directed fluorination

ABSTRACT

In this communication, we present an unusual bifurcated hydrogen bonding array between an OH donor and two C-F bond acceptors. This serendipitously discovered model system was observed in several substrates with various electron demands placed on the OH acceptor, and all show a symmetrical C—OH—$(F\text{-}C)_2$ hydrogen bonding interaction. We employ NMR and IR spectroscopy, X-ray crystallography and DFT theory to characterize this interesting and potentially biochemically relevant hydrogen bonding format.

1. Introduction

Nowadays it is well established that C-F bonds can serve as hydrogen bond acceptors, a fact whose relevance is emerging in synthetic, biological, and medicinal chemistry [1]. A common H-bond donor to covalent fluorine is the hydroxy group [2]. Although there is no doubt that such H-bonds meet a minimal energetic threshold, the resulting interactions are generally fairly weak. We reported one unusual exception some years back of a strong C-F—H—O bond locked within a cage framework [3]. Another way to strengthen the interaction is through a bifurcated system, and here the precedents are less numerous (Fig. 1). In one salient example, theoretical calculations [4], followed by gas-phase electron diffraction experiments, have provided evidence for a bifurcated conformer in 2-trifluoromethyl phenol [5]. The most abundant data in favor of bifurcation in this category are crystallographic interactions between hydroxy groups and vicinal C-F bonds of C_6F_5-groups; the shortest distances observed (with suitable refinement) are generally 2.4–2.6 Å [6]. To our knowledge, these types of bifurcated systems are generally not well characterized spectroscopically. In this paper, we present a serendipitously discovered, idealized model system that reveals a symmetrical C—OH—$(F\text{-}C)_2$ hydrogen bonding interaction, and characterize it through NMR and IR spectroscopy, X-ray crystallography, and DFT theory.

2. Results and discussion

Fig. 2 shows a spatial array of close C-F—H—O contacts derived from a CCDC search. As can be seen, a very wide range of geometrical orientations is present, giving us an expansive purview in the choice of a model system. The synthesis of our (accidental) candidate began with tertiary alcohol **1** [7], derived from bicyclo[3.3.1]nonan-1-one (Scheme 1) [8]. To our surprise, **1** (R = Cl) undergoes a highly diastereoselective directed difluorination to produce **2** in 55% yield. It was immediately apparent to us that **2** should potentially possess a very favorable bifurcated hydrogen bonding array as a result of its quasi-cage like structure.

The first order of business in the characterization of candidate **2** was an NMR study. ^{1}H NMR spectra revealed a downfield-shifted hydroxy proton (3.28 ppm) in the form of a well-defined triplet (J_{HF} = 9.60 Hz). Most notable was the reluctance of this proton to undergo fast exchange in the presence of saturated water in CH_2Cl_2, whereas its precursor **1** does so readily under identical conditions. Comparison of the ^{1}H NMR spectra of analogues shows some interesting features (Fig. 3). Whereas the hydroxy resonances of **4b, 5b**, and **2** show clear triplets, **6b**, substituted with an electron-withdrawing trifluoromethyl group, displays a broad singlet, indicative of fast exchange on the NMR time-scale.

Next, we characterized candidate **2** through X-ray crystallography. Single crystals of **2** were grown from the slow evaporation of a CH_2Cl_2 solution. As we anticipated, the structure reveals a bifurcated H-bond array, although curiously, it is not *perfectly* symmetrical (2.28 Å to F1, 2.08 Å to F2, Fig. 4). We interpret this result as a simple crystal packing phenomenon. The calculated structure of **2** (M06–2X/6–311++*G***) predicts perfect bifurcation (2.17 Å to F1 and F2). In any case, the interaction is substantial, and intermolecular hydrogen bonding is not observed in the crystal.

* Corresponding author.
E-mail address: lectka@jhu.edu (T. Lectka).
[1] Department of Chemistry and Biochemistry, Messiah University, 1 University Avenue, Mechanicsburg, PA, 17055, United States

https://doi.org/10.1016/j.jfluchem.2023.110104
Received 30 November 2022; Received in revised form 14 February 2023; Accepted 14 February 2023
Available online 26 February 2023

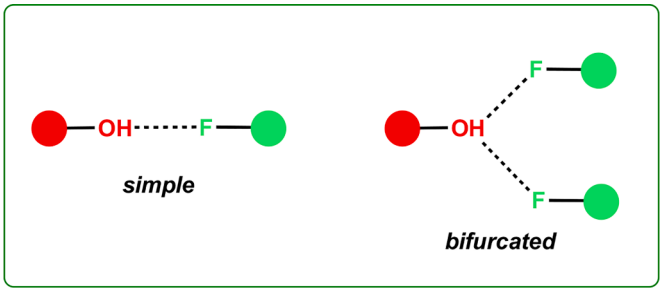

Fig. 1. Hydrogen bond types.

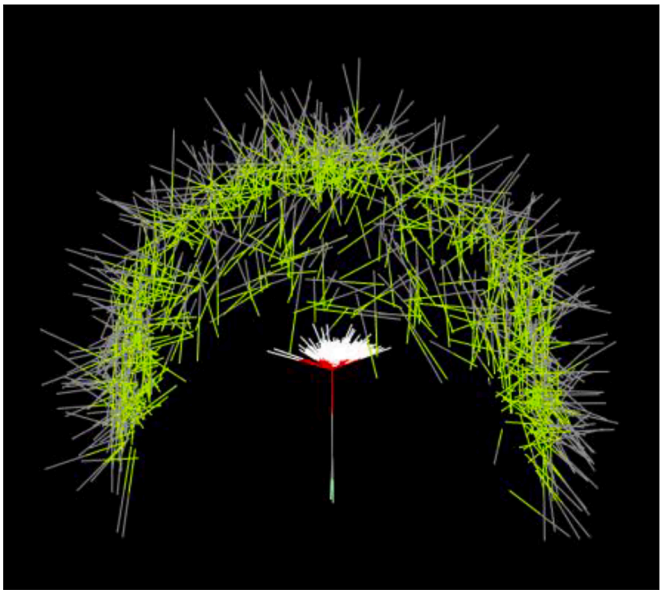

Fig. 2. Graphical CSD survey of C-F—H—O contacts (van der Waals radii – 0.30 Å). Light green lines denote C-F bonds near the fluorine atom terminus; gray atoms C-F bonds near the C atom terminus; white lines O—H bonds near the H atom terminus; red O—H bonds near the O atom terminus. O—H distances are normalized to the standard neutron diffraction value; oxygen atoms are overlaid.

An inspection of the crystal packing diagram of **2** shows the presence of secondary π-stacking, with secondary ordered interactions between C-F and C—H bonds (Fig. 5). The acidic proton of the hydroxy group engages in hydrogen bonding strictly intramolecularly, which is consistent

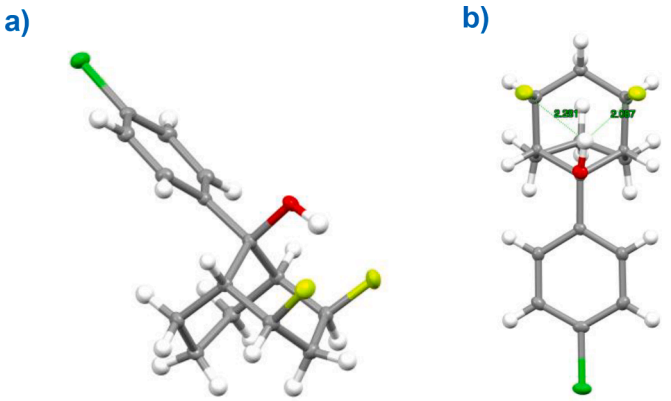

Fig. 4. a) Crystal structure of **2** (50% thermal ellipsoids). b) Slightly off-center bifurcation due to crystal packing effects.

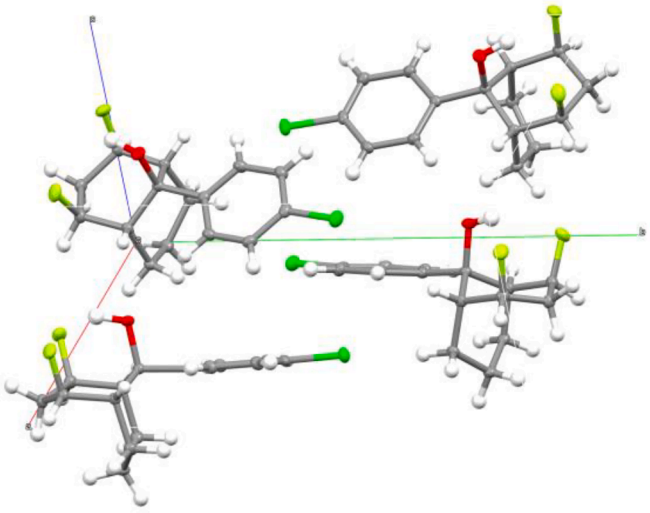

Fig. 5. Crystal packing diagram of **2** (50% thermal ellipsoids).

with our solution exchange studies. The crystallographic literature provides a number of examples of bifurcation in fluorinated alcohols; two examples are shown in Fig. 6. The first (left) exhibits a weak interaction between the OH and CF_3 groups in a hydrate [9]; the second is an interesting sandwich of intermolecular bifurcated arrays [10]. Steric hindrance around the tertiary alcohol and the proximity of the

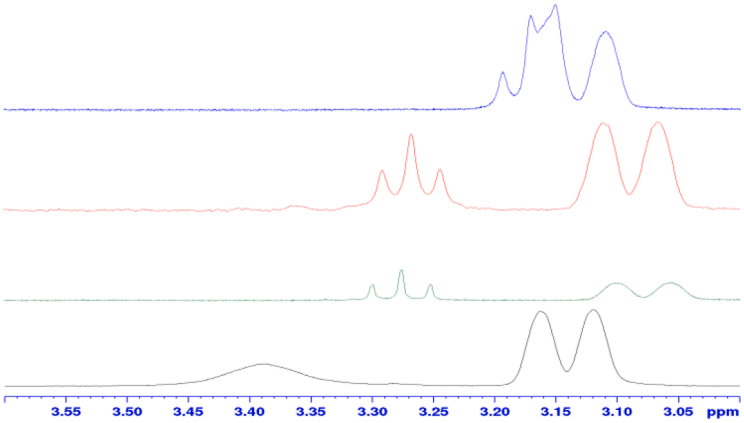

Fig. 3. O—H resonances in the ^{1}H NMR for the difluorinated compounds. Blue: phenyl substitution (**4b**), Red: fluorophenyl substitution (**5b**), Green: chlorophenyl substitution (**2**), Black: trifluoromethyl substitution (**6b**).

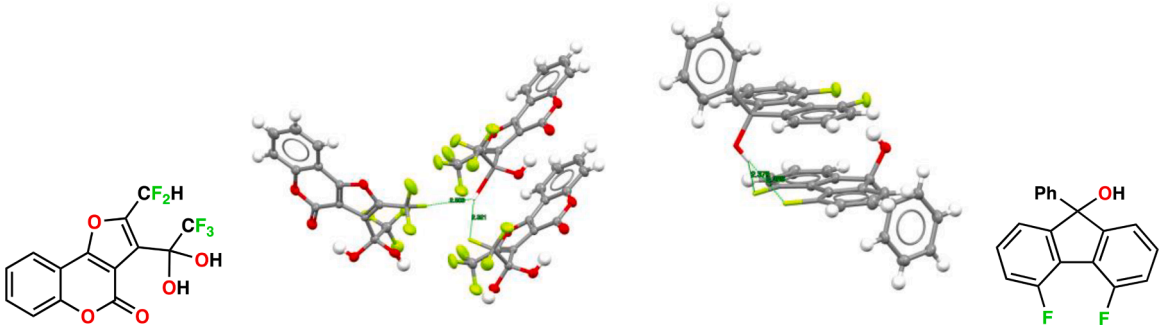

Fig. 6. Two examples of bifurcation in published crystal structures (50% thermal ellipsoids).

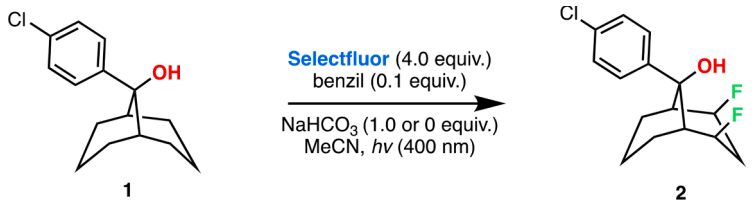

Scheme 1. Synthesis of candidate **2**.

fluorine atoms to the hydroxy group are deemed as the key reasons why the C—OH—$(F\text{-}C)_2$ hydrogen bonding diad forms [11,12].

Having fully characterized the chloro compound **2**, we sought to prepare a series of difluorinated compounds with a range of substituents at the para position of the aromatic ring. The parent phenyl compound, as well as the fluoro, trifluoromethyl, and t-butyl bicyclic alcohols, were each obtained through Grignard reactions with bicyclo[3.3.1]nonan-1-one (**3a-6a**). The nitro derivative (**7a**) was obtained by oxidation of the dimethylamino derivative (**8a**), which itself was obtained through a Grignard reaction. Additional electron-donating substitutions were not examined due to their preference for either benzylic radical fluorination or fluorination on the aromatic ring.

Difluorination occurred in a similar fashion on the parent phenyl substrate, as well as those containing F and CF_3. However, the reaction did not occur with either the t-butyl or nitro substituents (Scheme 2). When correlated to Hammett substituent constants, it appears that the OH in the parent compound is capable of directing fluorination to the ring when the substituent has a σ in the range of 0 (R = H) to 0.54 (R = CF_3). The strongly electron-withdrawing nitro group apparently pulls too much electron density from the OH for it to facilitate the coordination of Selectfluor. Much to our surprise, the t-butyl derivative, at the other end of the electron-demand continuum in our experiments, also did not undergo fluorination.

A significant amount of information was gleaned from an infrared (IR) analysis that, perhaps surprisingly, showed the OH stretches of **2** in the solid to be blue-shifted with respect to **1**. This result is indicative of an *intramolecular* H-bonding array in which fluorine is the acceptor atom and is consistent with observed crystal form which reveals no intermolecular H-bonding interactions. As a point of comparison, each of the spectra of the substrate molecules exhibits a set of OH stretches, one ranging from 3534 to 3583 cm^{-1}, and the other from 3373 to 3460 cm^{-1}. This result is characteristic of the solid phase IR spectra of many tertiary alcohols that are effectively dimerized in the crystal. On the other hand, the IR spectra of the difluorinated probe molecules are characterized by the total disappearance of the intermolecular hydrogen bonding OH band, as summarized in Table 1. The OH stretches in the probes are all observed within 11 cm^{-1} of one another, with the shift greatest for **5b**, which contains a fluoro group. Likewise, the C-F stretches are observed within a narrow range of 1072–1078 cm^{-1}. DFT calculations (ωB97xd/6–311++*G***) predict a firm red shift trend of about 25 cm^{-1} in going from free **4a-6a**, to intermolecular hydrogen bound **4b-6b**. Thus, the question of red versus blue shift is wholly dependent on the choice of reference (Scheme 3).

Likewise, in similar fashion to the chlorophenyl molecule **2**, each difluorinated compound exhibited a downfield O—H shift (Table 2). In three cases, clean triplets were observed ($J_{H\text{-}F}$ ranging from 9.6 to 10.4 Hz). These coupling constants were well reproduced by theory (ωB97xd/6–311++*G***).

Table 1
Infrared O—H and C-F stretches for substrates and difluorinated products. All data provided in cm^{-1}.

Substituent	Hammett constant	Substrate O—H stretches	Product O—H stretches	Product C-F stretches
H (**4b**)	0	3447, 3565	3611	1074
F (**5b**)	0.06	3463, 3534	3605	1072
Cl (**2**)	0.23	3373, 3426, 3558	3605	1073
CF_3 (**6b**)	0.54	3416, 3583	3599	1078

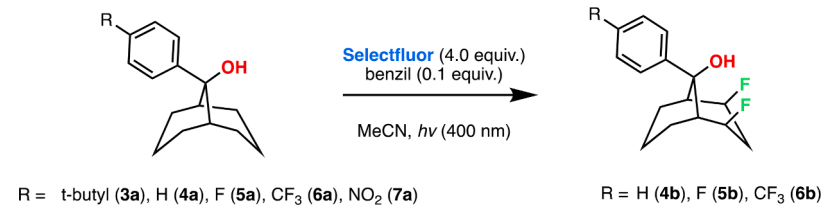

R = t-butyl (**3a**), H (**4a**), F (**5a**), CF_3 (**6a**), NO_2 (**7a**) R = H (**4b**), F (**5b**), CF_3 (**6b**)

Scheme 2. Synthesis of difluorinated bicyclic alcohols.

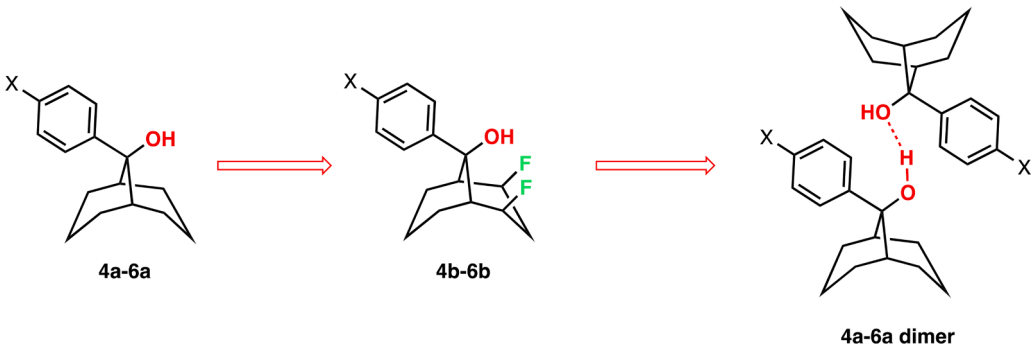

Scheme 3. Red shift trends in the infrared O—H and C-F stretches for parent (**4a-6a**) and difluorinated compounds (**4b-6b**). All data provided in cm^{-1}. With monomeric substrate alcohols as the baseline, fluorination produces a red shift due to the bifuracated bond, and crystallization of substrates **4a-6a** produces solid state dimerization and the largest red shift.

Table 2
^{1}H NMR chemical shifts and coupling constants for hydroxy groups of the difluorinated compounds.

Substituent	Chemical shift product OH (ppm)	OH-F coupling constant (Hz)
H (**4b**)	3.15	10.4
F (**5b**)	3.27	9.4
Cl (**2**)	3.28	9.6
CF_3 (**6b**)	3.39	–

An AIM (atoms in molecules) analysis of **2** reveals two bond critical points between the fluorine and hydrogen atoms (ρ = 0.0165 e, ρ = 0.0161 e), consistent with typical weak H-bond interactions [13].

Finally, we note that the heteroatomic functional group array of **2** resembles a rare *cis-cis*-1,3-difluoro-5-hydroxy-cyclohexane motif. *cis*-Polyfluorinated ("Janus-face") cyclohexanes are of interest in materials chemistry and drug discovery, wherein their packing arrangements show ordered layers of nonbonded C-F—H—C interactions. In a recent study, O'Hagan et al. showed that microbial hydroxylation of the Janus-face all cis-tetrafluorophenylcyclohexane leads to the installation of oxygen anti to the fluorine substituents [14], in contrast to our system, wherein fluorination proceeds in a syn fashion (Scheme 4).

3. Conclusions

In summary, we have characterized an interesting symmetrical intramolecular bifurcated hydrogen bonding array between an OH donor and two C-F bond acceptors. Several analogues possessing differential electron demands on the OH acceptor also show a symmetrical C—OH—$(F\text{-}C)_2$ hydrogen bonding diad. We employed NMR and IR spectroscopy, DFT theory, and X-ray crystallography to characterize the interaction in a thorough manner.

4. Experimental section

4.1. General information

Unless otherwise stated, all reactions were carried out under strictly anhydrous conditions and an N_2 atmosphere. All solvents were dried and distilled by standard methods. All other reagents were used as purchased, without further purification. ^{1}H spectra were acquired on a 400 MHz Bruker NMR spectrometer in d_3–MeCN or $CDCl_3$, ^{19}F spectra were acquired on a 400 MHz NMR spectrometer in $CDCl_3$, and ^{13}C NMR spectra were acquired on a 400 MHz NMR spectrometer in $CDCl_3$. The ^{1}H and ^{13}C NMR chemical shifts are given in parts per million (δ) with respect to an internal tetramethylsilane (TMS, δ = 0.00 ppm) standard. ^{19}F spectra are reported with respect to $CFCl_3$. NMR data are reported in the following format: chemical shift (multiplicity (*s* = singlet, *d* = doublet, *t* = triplet, *q* = quartet, *m* = multiplet), coupling constants (Hz). Spectral data were processed with Bruker Top Spin software. Infrared spectra were acquired on a ThermoScientific Nicolet iS5 spectrometer with an iD5ATR insert, at 4 cm^{-1} resolution. Photochemical reactions were run in front of a 72-LED work light (Designers Edge L1923). Column purification (if necessary) was conducted on a Teledyne Isco CombiFlash EZ Prep system using a Dynamax-60A SiO_2 column and HPLC grade EtOAc and hexanes. The Gaussian '09 package was used for all calculations [15]. All reflection intensities were measured at 110(2) K using a SuperNova diffractometer (equipped with Atlas detector) with Mo *Kα* radiation (λ = 0.71073 Å) under the program CrysAlisPro (Version CrysAlisPro 1.171.39.29c, Rigaku OD, 2017). The same program was used to refine the cell dimensions and for data reduction. The structure was solved with the program SHELXS-2018/3 (Sheldrick, 2018) and was refined on F^2 with SHELXL-2018/3 (Sheldrick, 2018). Numerical absorption correction based on gaussian integration over a multifaceted crystal model was applied using CrysAlisPro. The temperature of the data collection was controlled using the system Cryojet (manufactured by Oxford Instruments). The H atoms were placed at calculated positions (unless otherwise specified) using the instructions AFIX 13, AFIX 23 or AFIX 43 with the isotropic displacement parameters having values 1.2 U_{eq} of the attached C atoms. The H atom attached to O1 was found from difference Fourier map, and its coordinates were refined pseudofreely using the DFIX instruction in order to keep the $O-H$ distance to be consistent with the distance obtained from the DFT model. The structure is ordered. The absolute configuration has been established by anomalous-dispersion effects in diffraction measurements on the crystal, and the Flack and Hooft parameters refine to −0.004(14) and −0.006(12), respectively [16].

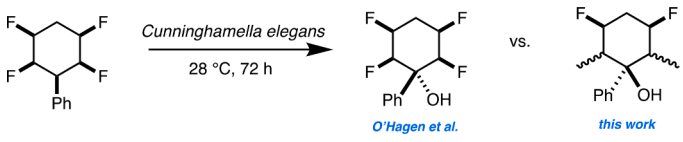

Scheme 4. Metabolism of "Janus-faced" polyfluorinated cyclohexanes leading to trans-hydroxy arrays.

4.2. General procedure for Grignard preparation of 1, 4a, and 8

To a flame-dried three-neck round-bottom flask equipped with a stir bar, additional funnel and condenser, under N_2, was added a suspension of bicyclo[3.3.1]nonan-9-one (0.200 g, 1.45 mmol) in dry THF (4.0 mL). The reaction mixture was cooled to 0 °C and 3 to 4 equivalents of the Grignard reagent was added dropwise (1 M 4-chlorophenyl magnesium bromide in Et_2O, 3 M phenyl magnesium bromide in Et_2O, or 2.5 M para-dimethylaminophenylmagnesium bromide in THF). The reaction mixture was slowly warmed to room temperature over 5 h and gently refluxed overnight. The reaction mixture was quenched with 1 M HCl

and extracted into CH_2Cl_2 repeatedly. The combined organic layers were washed with brine, dried with $MgSO_4$, filtered, and concentrated. The crude residue was purified through gradient column chromatography with EtOAc and hexanes.

4.3. General procedure for Grignard preparation of 3a, 5a and 6a

To a flame-dried three-neck round-bottom flask equipped with a stir bar, additional funnel, and condenser, under N_2, was added magnesium turnings (0.175 g, 7.30 mmol) and a crystal of I_2. The aromatic bromide (3.6 mmol) was dissolved in 15 mL THF. A small portion was added to the magnesium to initiate the reaction, with the remainder then added dropwise. The mixture was refluxed for 3 h. Bicyclo[3.3.1]nonan-9-one (0.200 g, 1.45 mmol) was dissolved in 2 mL THF and added dropwise. The mixture was gently refluxed overnight. The reaction mixture was quenched with 1 M HCl and extracted into CH_2Cl_2 repeatedly. The combined organic layers were washed with brine, dried with $MgSO_4$, filtered, and concentrated. The crude residue was purified by gradient column chromatography with EtOAc and hexanes.

4.4. General fluorination procedure

Selectfluor (180 mg, 0.50 mmol), and benzil (5.0 mg, 0.025 mmol) were added to an oven-dried μω-vial equipped with a stir bar; the vial was then sealed with a cap with a septum using a crimper and evacuated/refilled with N2 multiple times. The substrate (0.25 mmol) was dissolved in anhydrous CH3CN (4 mL) and added to the reaction vial, and the reaction mixture was irradiated with a cool white LED work light while stirring. After 3 h, an additional aliquot of Selectfluor (180 mg, 0.50 mmol) and benzil (5.0 mg, 0.25 mmol) in 4 mL CH3CN was added to the reaction mixture. After a total of 14 h, a 0.3 mL aliquot was taken for 19F NMR yield determination, and the rest of the reaction mixture was transferred to a separatory funnel, diluted with H2O, and extracted into CH2Cl2. The combined organic layers were washed with H2O and brine, then dried with MgSO4, filtered and concentrated. The crude reaction mixture was purified through gradient column chromatography on silica gel eluting with EtOAc and hexanes.

(1R,5S)−9-(4-chlorophenyl)bicyclo[3.3.1]nonan-9-ol (**1**). Yield 52%. White solid. IR (neat) cm^{-1}: 3558.4, 3425.61 and 3373.1, 2915.6, 1591.5, 1489.7, 1094.6, 1009.0, 862.4 and 825.2). ^1H NMR (400 MHz, $CDCl_3$): δ 7.46 (d, J = 8.4, 2H), 7.33 (d, J = 8.4, 2H), 2.46 (b, 2H), 2.39–2.30 (m, 2H), 1.99–1.57 (m, 9H), 1.57 (s, 1H), 1.33–1.30 (m, 1H). $^{13}C\{1H\}$ NMR (100.6 MHz, $CDCl_3$): δ 143.6, 133.1, 128.9, 127.2, 74.0, 35.5, 29.7, 27.2, 21.0, 20.6. FTMS (ESI) m/z $C_{15}H_{19}OCl$: calc 250.1124, observed 233.1086 (corresponds to loss of -OH).

(1R,2R,4S,5S,9 s**)−9-(4-chlorophenyl)−2,4-difluorobicyclo[3.3.1]nonan-9-ol** (**2**). Yield 43%. White solid. IR (neat) cm^{-1}: 3604.7, 2934.6, 1593.9, 1072.8, 1040.4, 883.1, 824.7. ^1H NMR (400 MHz, $CDCl_3$): δ 7.47 (d, J = 8.8, 2H), 7.38 (m, J = 8.4, 2H), 5.06 (dd, J = 48.1, 5.81 Hz, 2H), 3.28 (t, J = 9.6 Hz, 1H), 3.08 (d, J = 17.1 Hz, 2H), 2.78–2.37 (m, 2H), 1.83–1.71 (m, 2H), 1.62–1.56 (m, 2H), 1.37–1.30 (m, 1H), 1.27–1.13 (m, 1H). $^{13}C\{1H\}$ NMR (100.6 MHz, $CDCl_3$): δ 141.5, 133.4, 129.0, 127.2, 93.56 (d, J = 170.7 Hz) 73.4, 40.6 (d, J = 17.1 Hz) 34.8 (t, J = 23.2 Hz), 25.6 (d, J = 10.3 Hz), 17.6. ^{19}F NMR (376.5 MHz, $CDCl_3$): δ −152.81 (m). FTMS (ESI) m/z $C_{15}H_{17}OClF_2$: calc 286.0986, observed 269.0900 (corresponds to loss of -OH).

(1R,5S)−9-(4-(*tert*-butyl)phenyl)bicyclo[3.3.1]nonan-9-ol (3a). Yield 71%. White solid. IR (neat) cm^{-1}: 3533.7, 3465.8, 3416.4, 2917.7, 1511.4, 1037.1, 865.6, 829.2. ^1H NMR (400 MHz, $CDCl_3$): δ 7.50 (d, J = 9.2, 2H), 7.42 (d, J = 7.6, 2H), 2.53 (b, 2H), 2.49–2.37 (m, 2H), 2.05–1.62 (m, 10H), 1.45 (b, 1H), 1.37 (s, 9H). $^{13}C\{1H\}$ NMR (100.6 MHz, $CDCl_3$): δ 150.1, 142.0, 125.6, 125.3, 74.2, 35.5, 34.5, 31.4, 29.9, 27.3, 21.1, 20.7. FTMS (ESI) m/z $C_{19}H_{28}O$: calc 272.4320, observed 255.2100 (corresponds to loss of -OH).

(1R,5S)−9-phenylbicyclo[3.3.1]nonan-9-ol (4a). Yield 76%. White solid. IR (neat) cm^{-1}: 3564.6, 3447.2, 2914.5, 1397.7, 1011.6, 768.8, 698.4. ^1H NMR (400 MHz, $CDCl_3$): δ 7.56 (d, J = 8.8, 2H), 7.39 (t, J = 7.4, 2H), 7.29 (t, J = 6.2, 1H), 2.55 (b, 2H), 2.44–2.34 (m, 2H), 2.02 – 1.59 (m, 9H), 1.36–1.30 (m, 2H). $^{13}C\{1H\}$ NMR (100.6 MHz, $CDCl_3$): δ 145.0, 128.8, 127.3, 125.6, 74.4, 35.4, 29.7, 27.3, 21.1, 20.8. TOF-MS (ESI) m/z $C_{15}H_{20}O$: calc 216.1514, observed 216.1517.

(1R,2R,4S,5S,9 s**)−2,4-difluoro-9-phenylbicyclo[3.3.1]nonan-9-ol (4b).** Yield 24%. White solid. IR (neat): 3610.9, 2934.6, 1073.5, 1041.7, 766.8, 697.6. ^1H NMR (400 MHz, $CDCl_3$): δ 7.55 (d, J = 8.4, 2H), 7.43 (t, J = 7.8, 2H), 7.31 (t, J = 7.4, 1H), 5.05 (dd, J = 47.8, 5.8, 2H), 3.17 (t, J = 10.4, 1H), 3.15 (m, 2H), 2.79–2.41 (m, 2H), 1.88–1.77 (m, 2H), 1.62–1.55 (m, 2H), 1.37–1.12 (m, 2H). $^{13}C\{1H\}$ NMR (100.6 MHz, CDCl3): δ 142.9, 129.0, 127.7, 125.6, 93.7 (d, J = 170.0), 73.8, 40.6 (d, J = 13.1), 34.9 (t, J = 23.7), 25.8 (d, J = 16.1), 17.7. ^{19}F NMR (376.5 MHz, CDCl3): δ −152.20 (m). TOF-MS (ESI) m/z $C_{15}H_{18}OF_2$: calc 252.1326, observed 252.1318.

(1R,5S)−9-(4-fluorophenyl)bicyclo[3.3.1]nonan-9-ol (5a). Yield 50%. White solid, IR (neat) cm^{-1}: 3533.7, 3462.7, 2922.1, 1606.7, 1511.6, 1012.4, 832.5. ^1H NMR (400 MHz, $CDCl_3$): δ 7.51 (dd, J = 8.0, 5.2, 2H), 7.05 (t, 8.2, 2H), 2.48 (b, 2H), 2.41–2.31 (m, 2H), 1.20 – 1.57 (m, 9H), 1.44 (b, 1H), 1.39–1.29 (m, 1H). $^{13}C\{1H\}$ NMR (100.6 MHz, $CDCl_3$): δ 161.9 (d, J = 236.0), 140.9, 127.4 (d, J = 9.1), 115.4 (d, J = 19.1), 74.0, 35.6, 29.7, 27.2, 21.0, 20.6. ^{19}F NMR (376.5 MHz, $CDCl_3$): δ −114.93. TOF-MS (ESI) m/z $C_{15}H_{19}OF$: calc 234.1420, observed 234.1420.

(1R,2R,4S,5S,9 s**)−2,4-difluoro-9-(4-fluorophenyl)bicyclo[3.3.1]nonan-9-ol (5b).** Yield 35%. White solid. IR (neat): 3604.7, 2956.2, 1603.6, 1512.4, 1071.7, 883.0, 858.6. ^1H NMR (400 MHz, $CDCl_3$): δ 7.52 (dd, J = 9.6, 5.2, 2H), 7.10 (t, J = 8.8, 2H), 5.05 (dd, J = 48.6, 6.2, 2H), 3.27 (t, J = 9.4, 1H), 3.11–3.07 (m, 2H), 2.79–2.38 (m, 2H), 1.85–1.58 (m, 3H), 1.39–1.13 (m, 3H). $^{13}C\{1H\}$ NMR (100.6 MHz, $CDCl_3$): δ 162.0 (d, J = 258.5), 138.8, 127.5 (d, J = 8.0), 115.7 (d, J = 22.1), 93.6 (d, J = 170.0), 73.3, 40.7 (d, J = 15.1), 34.8 (t, J = 21.1), 25.6 (d, J = 11.1), 17.6 ^{19}F NMR (376.5 MHz, $CDCl_3$): δ −114.93, −152.20 (m). TOF-MS (ESI) m/z $C_{15}H_{17}OF_3$: calc 270.1232, observed 270.1231.

(1R,5S)−9-(4-(trifluoromethyl)phenyl)bicyclo[3.3.1]nonan-9-ol (6a). Yield 84%. White solid, IR (neat) cm^{-1}: 3583.1, 3416.4, 2922.3, 1332.9, 1126.2, 864.4, 834.9. ^1H NMR (400 MHz, $CDCl_3$): δ 7.68 (m, 4H), 2.54 (b, 2H), 2.43–2.33 (m, 2H), 2.02–1.76 (m, 10H), 1.70–1.60 (m, 1H). $^{13}C\{1H\}$ NMR (100.6 MHz, $CDCl_3$): δ 149.0 (q, J = 1.3), 129.5 (q, J = 32.5), 126.1, 125.7 (q, J = 3.7), 124.1 (q, J = 270.6), 74.2, 35.4, 29.6, 27.2, 20.9, 20.6. ^{19}F NMR (376.5 MHz, $CDCl_3$): δ −62.12. TOF-MS (ESI) m/z $C_{16}H_{19}OF_3$: calc 284.1388, observed 284.1375.

(1R,2R,4S,5S,9 s**)−2,4-difluoro-9-(4-(trifluoromethyl)phenyl)bicyclo[3.3.1]nonan-9-ol (6b).** Yield 53%. White solid. IR (neat): 3598.6, 2962.4, 1329.7, 1077.7, 1067.3, 889.1, 838.3. ^1H NMR (400 MHz, $CDCl_3$): δ 7.68 (m, 4H), 5.08 (dd, J = 48.0, 6.0, 2H), 3.39 (b, 1H), 3.16–3.12 (m, 2H), 2.80–2.38 (m, 2H), 1.83–1.56 (m, 4H), 1.40–1.16 (m, 2H). $^{13}C\{1H\}$ NMR (100.6 MHz, $CDCl_3$): δ 146.7, 129.8 (q, J = 33.5), 126.2, 125.9, 124.0 (q, J = 283.4), 93.5 (d, J = 182.1), 73.6, 40.5 (d, J = 17.1), 34.9 (t, J = 22.6), 25.5 (d, J = 11.1), 17.5. ^{19}F NMR (376.5 MHz, $CDCl_3$): δ −62.81, −152.91 (m). TOF-MS (ESI) m/z $C_{16}H_{17}OF_5$: calc 320.1200, observed 303.1158 (corresponds to loss of -OH).

(1R,5S)−9-(4-nitrophenyl)bicyclo[3.3.1]nonan-9-ol (7a). Potassium iodide (12.4 mg, 0.07 mmol) and ammonium acetate (78.7 mg, 1.0 mmol) were added to a round-bottom flask. (1R,5S)−9-(4-(Dimethylamino)phenyl)bicyclo[3.3.1]nonan-9-ol (80.5 mg, 0.31 mmol) was dissolved in 10 mL CH_3CN and added to the flask. t-Butyl peroxide, 70% in water, (0.52 mL, 3.7 mmol) was added and the mixture was gently refluxed overnight. The reaction mixture was quenched with saturated $Na_2S_2O_3$ and extracted into EtOAc repeatedly. The combined organic layers were washed with brine, dried with Na_2SO_4, filtered, and concentrated. The crude residue was purified by gradient column chromatography with EtOAc and hexanes to yield 55% product as a white solid. IR (neat) cm^{-1}: 3558.4, 2922.3, 1594.4, 1508.2, 1350.2, 1040.4, 868.1, 850.1. ^1H NMR (400 MHz, $CDCl_3$): δ 8.22 (d, J = 14.0, 2H), 7.71 (d, J = 14.4, 2H), 2.53 (s, 2H), 2.41–2.32 (m, 2H), 2.01–1.61 (m, 9H), 1.39–1.21 (m, 2H). $^{13}C\{1H\}$ NMR (100.6 MHz, $CDCl_3$): δ 152.3, 147.0, 126.8, 123.9, 74.2, 35.5, 29.5, 27.1, 20.8, 20.4. TOF-MS (ESI) $m/$

z $C_{15}H_{19}NO_3$: calc 261.1365, observed 261.1373.

(1R,5S)−9-(4-(dimethylamino)phenyl)bicyclo [3.3.1] nonan-9-ol (8a). Yield: 80%. White solid. IR (neat) cm^{-1}: 3339.2, 2916.4, 1606.7, 864.9, 821.7. ^{1}H NMR (400 MHz, $CDCl_3$): δ 7.42 (d, $J = 16$, 2H), 6.75 (d, 12, 2H), 2.96 (s, 6H), 2.47 (b, 2H), 2.43–2.33 (m, 2H), 2.00–1.57 (m, 9H), 1.34–1.27 (m, 2H). ^{13}C{1H} NMR (100.6 MHz, $CDCl_3$): δ 149.6, 133.0, 126.5, 112.7, 74.1, 40.1, 35.6, 30.0, 27.5, 21.3. FTMS + p (ESI) *m/z* $C_{17}H_{25}NO$ + proton: calc 260.2016, observed 260.2000.

Associated content

Supporting Information. The Supporting Information containing experimental procedures, spectra, and computational data at DOI:

Notes

The authors declare no competing financial interest.

Declaration of Competing Interest

The authors declare the following financial interests/personal relationships which may be considered as potential competing interests:

Thomas Lectka reports financial support was provided by National Science Foundation.

Data Availability

Data will be made available on request.

Acknowledgment

T.L. thanks the National Science Foundation (NSF) (Grant no. CHE 2102116) for financial support. Mass spectral data were obtained at University of Delaware's mass spectrometry centers.

Supplementary materials

Supplementary material associated with this article can be found, in the online version, at doi:10.1016/j.jfluchem.2023.110104.

References

[1] a) B.K. Park, N.R. Kitteringham, P.M. O'Neill, Metabolism of fluorine-containing drugs, Annu. Rev. Pharmacol. Toxicol. 41 (2001) 443–470;
b) N.A. Meanwell, Fluorine and fluorinated motifs in the design and application of bioisosteres for drug design, J. Med. Chem. 61 (2018) 5822–5880;
c) W.K. Hagmann, The many roles for fluorine in medicinal chemistry, J. Med. Chem. 51 (2008) 4359–4369.
[2] a) P. Murray-Rust, W.C. Stallings, C.T. Monti, R.K. Preston, J.P. Glusker, Intermolecular interactions of the C-F Bond: the crystallographic environment of fluorinated carboxylic acids and related structures, J. Am. Chem. Soc. 105 (10) (1983) 3206–3214;
b) H. Takemura, M. Kotoku, M. Yasutake, T. Shinmyozu, 9-Fluoro-18-hydroxy-[3.3]metacyclophane: synthesis and estimation of a C-F···HO hydrogen bond, Eur. J. Org. Chem. (2004) 2019–2024.
[3] a) G.H. Holl, C.R. Pitts, T. Lectka, Fluorine in a C-F bond as the key to cage formation, Angew. Chem. Int. Ed. 57 (2018) 2–11;
b) M.D. Struble, C. Kelly, M.A. Siegler, T. Lectka, Search for a strong, virtually "No-shift" hydrogen bond: a cage molecule with an exceptional OH···F interaction, Angew. Chem. Int. Ed. 53 (2014) 8924–8928.
[4] A. Kovác, I. Kolossváry, G.I. Csonka, I. Hargittai, Theoretical study of intramolecular hydrogen bonding and molecular geometry of 2-trifluormethylphenol, J. Comput. Chem. 17 (1996) 1804–1819.
[5] A. Kovác, I. Hargittai, Bifurcated hydrogen bonding in 2-trifluoromethylphenol confirmed by gas electron diffraction, Phys. Chem. A. 102 (1998) 3415–3419.
[6] C.R. Groom, I.J. Bruno, M.P. Lightfoot, S.C. Ward, The Cambridge structural database, Acta Cryst. (2016) 171–179. *B72*.
[7] S.A. Harry, M.R. Xiang, E. Holt, A. Zhu, F. Ghorbani, D.;. Patel, T. Lectka, Hydroxy-directed fluorination of remote unactivated C(sp^3)-H bonds: a new age of diastereoselective radical fluorination, Chem. Sci. 13 (2022) 7007–7013.
[8] B.A. Carlson, H.C. Brown, Boranes in functionalization of dienes to cyclic ketones: bicyclo[3.3.1]nonan-9-one, Org. Synth. 58 (1978) 24.
[9] S.S. Vagh, B.-J. Hou, A. Edukondalu, P.-C. Wang, W. Lin, Phosphine-mediated MBH-type/acyl transfer/wittig sequence for construction of functionalized Furo [3,2-*c*]coumarins, Org. Lett. 23 (2021) 842–846.
[10] R. Deng, J. Xi, Q. Li, Z. Gu, Enantioselective C-C bond cleavage for biaryl atropisomers synthesis, Chem. 5 (2019) P1834–P1846.
[11] C.P. Brock, L.L. Duncan, Anomalous space-group frequencies for monoalcohols C_nH_mOH, Chem. Mater. 6 (1994) 1307–1312.
[12] R. Taylor, C.F. Macrae, Rules governing the crystal packing of mono- and dialocohols, Acta Cryst. (2001) 815–827. *B57*.
[13] U. Koch, P.L.A. Popelier, Characterization of C-H-O hydrogen bonds on the basis of the charge density, J. Phys. Chem. 99 (1995) 9747–9754.
[14] A. Rodil, S. Bosisio, M.S. Ayoup, L. Quinn, D.B. Cordes, A.M.Z. Slawin, C. D. Murphy, J. Michel, D.O. O'Hagan, Metabolism and hydrophilicity of the polarised 'Janus face' all-*cis* tetrafluorocyclohexyl ring, a candidate motif for drug discovery, Chem. Sci. 9 (2018) 3023–3028.
[15] Gaussian 09, Revision A.1, M.J. Frisch, et al. Gaussian, Inc., Wallingford, CT.
[16] G.M. Sheldrick, Crystal structure refinement with SHELXL, Acta Cryst (2015) 3–8. *C71*.